Biomaterials Science

In vitro vascularization of tissue engineered constructs by non-viral delivery of pro-angiogenic genes

Journal:	*Biomaterials Science*
Manuscript ID	BM-ART-09-2020-001560.R2
Article Type:	Paper
Date Submitted by the Author:	06-Jan-2021
Complete List of Authors:	Moreira, Helena; 3B's Research Group; ICVS/3B's – PT Government Associate Laboratory Raftery, Rosanne; Tissue Engineering Research Group, Dept. of Anatomy & Regenerative Medicine, Royal College of Surgeons in Ireland (RCSI); Trinity Centre for Biomedical Engineering, Trinity College Dublin (TCD); Advanced Materials and Bioengineering Research (AMBER) Centre, RCSI & TCD da Silva, Lucilia; 3B's Research Group; ICVS/3B's – PT Government Associate Laboratory Cerqueira, Mariana; University of Minho, ICVS; ICVS/3B's – PT Government Associate Laboratory Reis, Rui; 3B's Research Group; ICVS/3B's – PT Government Associate Laboratory Marques, Alexandra; 3B's Research Group; ICVS/3B's – PT Government Associate Laboratory O'Brien, Fergal; Royal College of Surgeons in Ireland, Anatomy; Trinity Centre for Biomedical Engineering, Trinity College Dublin (TCD); Advanced Materials and Bioengineering Research (AMBER) Centre, RCSI & TCD

ARTICLE

In vitro vascularization of tissue engineered constructs by non-viral delivery of pro-angiogenic genes

Received 00th January 20xx,
Accepted 00th January 20xx

DOI: 10.1039/x0xx00000x

Helena R. Moreira[a,b], Rosanne M. Raftery[c,d,e], Lucília P. da Silva[a,b], Mariana T. Cerqueira[a,b], Rui L. Reis[a,b], Alexandra P. Marques[a,b], Fergal J. O'Brien*[c,d,e]

Vascularization is still one of the major challenges in tissue engineering. In the context of tissue regeneration, the formation of capillary-like structures is often triggered by the addition of growth factors which are associated with high cost, bolus release and short half-life. As an alternative to growth factors, we hypothesized that delivering genes-encoding angiogenic growth factors to cells in a scaffold microenvironment would lead to a controlled release of angiogenic proteins promoting vascularization, simultaneously offering structural support for new matrix deposition. Two non-viral vectors, chitosan (Ch) and polyethyleneimine (PEI), were tested to deliver plasmids encoding for vascular endothelial growth factor (pVEGF) and fibroblast growth factor-2 (pFGF2) to human dermal fibroblasts (hDFbs). hDFbs were successfully transfected with both Ch and PEI, without compromising the metabolic activity. Despite low transfection efficiency, superior VEGF and FGF-2 transgene expression was attained when pVEGF was delivered with PEI and when pFGF2 was delivered with Ch, impacting the formation of capillary-like structures by primary human dermal microvascular endothelial cells (hDMECs). Moreover, in a 3D microenvironment, when PEI-pVEGF and Ch-FGF2 were delivered to hDFbs, cells produced functional pro-angiogenic proteins which induced faster formation of capillary-like structures that were retained in vitro for longer time in a Matrigel assay. The dual combination of the plasmids resulted in a downregulation of the production of VEGF and an upregulation of FGF-2. The number of capillary-like segments obtained with this system was inferior to the delivery of plasmids individually but superior to what was observed with the non-transfected cells. This work confirmed that cell-laden scaffolds containing transfected cells offer a novel, selective and alternative approach to impact the vascularization during tissue regeneration. Moreover, this work provides a new platform for pathophysiology studies, models of disease, culture systems and drug screening.

Introduction

The vascularization of tissue-engineered constructs is still one of the major challenges of the field.[1] Considering vascularization takes place in a highly complex and regulated microenvironment, if a tissue-engineered construct is not able to integrate with surrounding tissues and establish interconnections to host blood vessels after implantation, diffusion of oxygen and nutrients supply becomes limited, resulting in loss of cell viability at the core of the construct, and ultimately, graft failure.[2]

Pre-vascularization by culturing endothelial cells on a scaffold prior to implantation is one of the main strategies used to promote vascularization through the inosculation of pre-formed and host vessel-like structures.[3] To date, the majority of pre-vascularization strategies rely on the use of endothelial cells in co-culture with perivascular cells.[4] However, one of the major limitations of this approach is the cell source and availability of mature/progenitor endothelial cells.[5] Human pluripotent stem cells and human mesenchymal stem cells have also been used,[6] but protocols for the differentiation towards endothelial cells are still not sufficiently robust. Additionally, external growth factors have also been used to develop microvascular networks.[6] The delivery of vascular endothelial growth factor (VEGF), basic fibroblasts growth factor (FGF-2) and/or platelet-derived growth factor, which mediate the recruitment, expansion and survival of endothelial cells, as well as tubule formation and stabilization,[7–11] were also shown to be a powerful strategy to stimulate angiogenesis.[12–15] However, the use of growth factors is associated with several limitations that includes high cost, bolus release of proteins, short half-life, and the requirement of high doses to achieve a therapeutic effect,[16] which in the case of angiogenic factors can be linked to tumor development.[17] To tackle this, genes encoding for specific angiogenic proteins, can be delivered as plasmid DNA (pDNA) to

[a.] *3B's Research Group, I3Bs – Research Institute on Biomaterials, Biodegradables and Biomimetics, Headquarters of the European Institute of Excellence on Tissue Engineering and Regenerative Medicine, University of Minho, Avepark, Barco, 4805-017 Guimarães, Portugal*
[b.] *ICVS/3B's – PT Government Associate Laboratory, Braga/Guimarães 4805-017, Portugal*
[c.] *Tissue Engineering Research Group, Dept. of Anatomy & Regenerative Medicine, Royal College of Surgeons in Ireland (RCSI), Dublin, Ireland*
[d.] *Trinity Centre for Biomedical Engineering, Trinity College Dublin (TCD), Dublin, Ireland*
[e.] *Advanced Materials and Bioengineering Research (AMBER) Centre, RCSI & TCD, Dublin, Ireland*
Electronic Supplementary Information (ESI) available: [details of any supplementary information available should be included here]. See DOI: 10.1039/x0xx00000x

induce a sustained production of physiologically appropriate amounts of therapeutic protein, subsequently inducing the formation of stable capillary-like structures.

Viral and non-viral vectors can be used to deliver pDNA. However, non-viral vectors are generally safer, less immunogenic, and are more straightforward to mass-produce with high tunability when compared to viral vectors. [18] However they are typically limited by lack of efficacy due to low transfection efficiency. Recently, in a number of studies from our lab, chitosan (Ch)[19,20] and polyethyleneimine (PEI)[21,22] have been optimized as vectors demonstrating high transfection efficiency and uncompromised cell viability. The idea of combining cells transfected with non-viral vector and therapeutic genes and scaffolds is an innovative strategy that guarantees a sustainable protein production, while scaffolds offer structural support and a matrix for new tissue deposition and act as cell delivery devices.[16] Collagen (COL)-based scaffolds[23,24] and gellan gum (GG)-based spongy-like hydrogels[25,26] have been explored for a range of tissue engineering applications, including skin wound healing.[5,27] While COL-chondroitin sulfate (ChS) and GG-hyaluronic acid (HyA) were capable of supporting skin neo-tissue formation, it was also shown that cells and materials in those constructs synergize promoting neo-vascularization.[5,20] COL-HyA scaffolds were firstly developed for cartilage regeneration,[28] but have an enormous interest in the area of skin tissue engineering due to the importance of HyA in skin remodeling and angiogenesis.[29]

In this context, we hypothesized that the angiogenic and thus regenerative potential of collagen (COL)-glycosaminoglycans (GAG) scaffolds and gellan gum (GG)-based spongy-like hydrogels would be maximized when combined with cells transfected with genes encoding for angiogenic growth factors. The optimal vector for the delivery of plasmids encoding for VEGF (pVEGF) and for FGF-2 (pFGF2) for the downstream production of angiogenic factors by human dermal fibroblasts (hDFbs) was established. Subsequently the potential of engineering a novel cell-laden scaffold-based strategy for the in situ delivery of VEGF and FGF-2 was evaluated by seeding transfected hDFbs and human dermal microvascular endothelial cells (hDMECs) in COL-ChS, COL-HyA and GG-HyA to analyze the behavior of the endothelial cells.

Materials and Methods

Plasmid propagation & purification. Plasmid DNA encoding Gaussia Luciferase (pGLuc; New England Biolabs, USA), Green Fluorescent Protein (pGFP; Amaxa, Lonza, Germany), Vascular Endothelial Growth Factor (pVEGF; Genecopaeia, USA) and basic Fibroblast Growth Factor (pFGF2; kindly provided by Prof. Henning Madry from Saarland University) were propagated via the transformation of Subcloning Efficiency™ DH5α™ chemically competent Escherichia coli cells (Life Technologies, Ireland). All plasmid DNA were isolated and purified using an Endotoxin Free Maxi-prep Kit (Qiagen, UK) as per the manufacturer's instructions. The obtained plasmid was dissolved in Tris-EDTA buffer at a concentration of 0.5 µg µL-1 and stored at -20 ºC until further usage.

Non-viral vector-pDNA polyplex formation. Chitosan (Ch, Mw 7.3 kDa; DD > 97%; Novamatrix, FMC Biopolymer, Norway) nanoparticles were formulated by electrostatic interaction between cationic chitosan and anionic pDNA. Nanoparticles were allowed to equilibrate for 30 min at room temperature before use. The ratio of chitosan to pDNA (N/P ratio, nitrogen:phosphate ratio) was 10 and the pDNA loading dose was 0.33 µg as optimized previously.[19] Branched PEI (Sigma Aldrich, Ireland) was purified via dialysis. For this, PEI was dissolved in deionized water and loaded into Cellu-Sep H1 membranes (25 kDa MWCO). This was dialyzed against a 400-fold excess of deionized water a total of four times over night before the remaining PEI was lyophilized for use. 2 µg of pDNA was added to sterile molecular grade water followed by dropwise addition of PEI at a N/P ratio of 7 and 30 min equilibration at room temperature.[21]

Assessment of complexation efficiency. A SYBR® Safe (Life Technologies, Ireland) exclusion assay was used to assess how effectively Ch and PEI binds to the pDNA of interest. SYBR® Safe fluoresces strongly upon intercalation between the base pairs of pDNA. Upon complete and stable binding of Ch or PEI to pDNA, there should be no free pDNA available for intercalation with the probe and the fluorescent signal is quenched.[30,31] Ch-pDNA and PEI-pDNA nanoparticles were prepared as in Section 2.2 and then diluted to 1 mL with molecular grade 20 mM NaCl. 0.5 µL of SYBRSafe DNA stain was then added and the fluorescence signal read (RFU), in triplicate, on a spectrofluorimeter (Bio-Tek Synergy HT 188743, Fisher Scientific, Ireland) at an excitation wavelength of 488 nm and an emission wavelength of 522 nm. Binding efficiency was calculated following Equation 1, as follows.

Binding efficiency (%) = $100-[(RFU_{vector\text{-}pDNA} \times 100)/RFU_{pDNA}]$ (1)

Gel electrophoresis was also used to confirm complexation efficiency. For that, 5 µL of each non-viral vector-pDNA complex was added to 1 µL 6X loading dye (ThermoFisher) and run on a 1 % agarose (Lonza, Switzerland) gel for 45min, along with controls (pDNA alone, non-viral vector alone and a 10000bp ladder). The gels were viewed in the 600 channel of an Odyssey Fc Imaging System (LI-COR, US), and imaged and quantified using the Image Studio Software (LI-COR, US).

Human microvascular endothelial cells isolation and culture. Human microvascular endothelial cells (hDMECs) were harvested from human skin samples obtained from abdominoplasties performed at Hospital da Prelada (Porto, Portugal), after informed consent. Samples were obtained under a collaboration protocol with the 3B's Research Group, approved by the ethical committees of both institutions. Briefly, skin specimens were cut into small fragments and incubated overnight in dispase (2.4 U mL^{-1}) (BD Biosciences, USA) at 4 °C. hDMECs were obtained through the filtration and centrifugation of the dispase solution. The remaining skin pieces were discarded. hDMECs were cultured in 0.7 % gelatin (Sigma, USA) coated flasks with Endogro-MV VEGF (Millipore, USA). Cells were passaged at 70-90 % confluency and used at passage 3–4.

Human dermal fibroblast culture. Primary human dermal fibroblasts (hDFbs, ATCC, supplied by LGC Standards, UK) were expanded in Dulbecco's Modified Eagles Medium supplemented with 1 % penicillin/streptomycin, 10 % FBS (Labtech, UK), 1 % glutamax (Biosciences, Ireland). Cells were passaged at 70-90 % confluency and expanded to passage 6 for all experiments.

hDFbs monolayer transfection. hDFbs were seeded at a density of $2x10^4$ cells per well in 24 well adherent plates (Corning, Costar, Ireland). After 24 h, cells were washed with PBS and provided with 1 mL of OptiMEM (Gibco, Ireland). After 1 h, complexed nanoparticles were added in OptiMEM. After 5 h, transfection media was removed, cells were washed twice in PBS and growth medium was replenished. Prior to each time point (3, 5, 7, 10 and 14 days), the medium was removed and replaced by DMEM without FBS for a starvation period of 24 h. The supernatant was collected after 24 h for the ELISA assay and Matrigel assay.

Transfection efficiency assessment. Transfection efficiency was analyzed by quantifying luciferase luminescence intensity or by the quantification of GFP+ cells by flow cytometry and fluorescence microscopy. For the analysis of luciferase production at days 3, 7 and 14, 1 mL of complete medium was removed from each well and replaced with 1 ml of fresh media. Luciferase content was determined using a Pierce™ Gaussia Luciferase Flash Assay Kit (Thermo Scientific, Ireland) as per the manufacturer's instructions. Briefly, 20 µL of the collected media were transferred in triplicate to a black 96 well plate. 50 µL of the working solution was added to each well and luminescence was acquired using a Varioskan Flash multimode plate reader (Fisher Scientific, Ireland). Cells transfected with Chitosan-pGFP or PEI-pGFP were visualized using an Axio Observer inverted Microscope (Zeiss, Germany). All cells (transfected/non-transfected) were labelled with Phalloidin-TRITC (0.5 µg mL^{-1}, Sigma, Ireland) and DAPI (0.02 mg mL^{-1}, Biotium, USA) for visual confirmation. For flow cytometry analysis pGFP transfected hDFbs were analyzed in BD FACSAria III by BD FACSDIVA software (both BD Biosciences, Belgium) where GFP fluorescence was expressed as a percentage of GFP positive over the total number of gated cells.

Non-viral vector-pDNA toxicity assessment. To assess the toxicity of the vector-pDNA complexes, metabolic activity and cell proliferation were quantified at 3, 7 and 14 days post-transfection using CellTiter 96® AQueous One Solution Cell Proliferation Assay (Promega, USA) and Quant-iT PicoGreen dsDNA Assay Kit (Invitrogen, UK), respectively. At each time-point, after washing with PBS, cells were incubated with 20 µL of MTS solution (4:1 media:MTS) for three hours at 37 °C. Then, 100 µL of the supernatant was transferred in triplicate to a 96 well plate and the absorbance of each sample was read at 490 nm. Metabolic activity was normalized with the dsDNA obtained from the Quant-iT PicoGreen dsDNA Assay and data was expressed as a percentage cell metabolic activity in relation to the non-transfected hDFbs. Briefly, for the quantification of dsDNA, cells were incubated with 0.5 mL of ultra-pure water for 1 h at 37 ºC, collected and then frozen at -80 ºC. 28.7 µL of each cell lysate was added to each well of a white 96 well plate followed by the addition of 100 µL of 1x Tris-EDTA buffer and 78.3 µL of Picogreen reagent according to manufacturer's instruction. After a 10min incubation at RT, fluorescence was read at 480/520 nm using a Varioskan Flash multimode plate reader. The concentration of DNA present in each sample was determined against a standard curve.

Collagen-GAG scaffold fabrication. Collagen-GAG scaffolds were fabricated using a lyophilization technique developed by O'Brien et al.[23,24] COL-HyA or COL-ChS scaffolds were made by blending 1.8 g of bovine tendon collagen (Southern Lights Biomaterials, New Zealand) in 300 mL of 0.5 M glacial acetic acid (HOAc, Fisher Scientific, Ireland) for 90 min. A total of 0.16 g of glycosaminoglycan (hyaluronic acid sodium salt derived from Streptococcus equi or chondroitin sulfate sodium salt from shark cartilage, Sigma Aldrich, Ireland), was dissolved in 60 mL of 0.5M HOAc and added to the collagen slurry at a rate of 5 mL/10 min while blending at 15.000 rpm. The slurry was blended for a further 60 min following the addition of all of the GAG. Gas was removed from the slurries using a vacuum pump and freeze-dryed (Advantage EL, VisTir Co., Gardiner NY) to a final temperature of −10 °C using a controlled freezing rate of 1 °C per minute. Afterwards, the scaffold sheets were crosslinked dehydrothermally (DHT) at 105 ºC for 24 h at 0.05 bar in a vacuum oven (Vacucell 22; MMM, Germany). Scaffolds with a diameter of 5 mm were created using a biopsy punch, hydrated with PBS and chemical crosslinked using a mixture of 6 mM N-(3-Dimethylaminopropyl)-N'-ethylcarbodiimide hydrochloride (EDC) and 5.5 mM N-Hydroxysuccinimide (NHS).

Gellan gum-based scaffolds fabrication. Gellan gum (GG)-hyaluronic acid (HyA) spongy-like hydrogels were prepared as previously described.[25,26] Briefly, a solution of 0.44 % (w/V) hyaluronate (1.5 MDa, LifeCore Biomedical, USA)[32] and 0.5 % (w/V) gellan gum (Gelzan, Sigma-Aldrich, France) was prepared at 90 ºC. Additionally, 0.25 % (v/V) gellan gum chemically modified with divinyl sulfone (GGDVS)[33] was reacted with thiol-cyclo-RGD (800 µM, Cyclo(-RGDfC) 95 %, GeneCust Europe) for 1 h. Hydrogels were prepared by mixing the hyaluronate/gellan gum solution with GGDVSRGD and then caste into the desired molds. The hydrogel was progressively formed until room temperature was reached. Afterwards, hydrogels were frozen at -80 ºC overnight and then freeze-dried (Telstar, Spain) for 24 h to obtain GG-HyA dried polymeric networks. Spongy-like hydrogels were formed after rehydration of the dried polymeric networks.

Cell-laden scaffold fabrication. hDFbs were transfected with PEI-pVEGF N/P 7 (2 µg pDNA), Ch-pFGF2 N/P 10 (0.33 µg pDNA) or the dual combination PEI-pVEGF+Ch-pFGF2 (1 µg pVEGF + 0.165 µg pFGF2; P+C) for 5 h at 37 °C. After hDFbs transfection, hDFbs were mixed with hDMECs (1:4) and the cell suspension was seeded on the different scaffolds: COL-HyA, COL-ChS and GG-HyA. The scaffolds were incubated at 37 °C for 30 min and afterwards, 1 mL of a mix of DMEM and EndoGRO MV-VEGF (Millipore, Germany) (1:1) was added to each well. Prior each time point (3 and 7 days), the medium was removed and replaced by DMEM/EndoGRO MV-VEGF (1:1) without FBS and without growth factors for a starvation period of 24 h. The supernatant, or conditioned media, was collected after 24 h for the ELISA assay and Matrigel assay. Scaffolds were fixed with 10 % Formalin (Bio-Optic, Italy) for immunocytochemistry.

Enzyme-linked immunosorbent assay (ELISA) for VEGF and FGF-2 quantification post transfection. The levels of VEGF and FGF-2 secreted by the transfected cells were quantified by ELISA assays (R&D Systems, UK) in both 2D and 3D systems. Assays were carried out according to the manufacturer's instructions and the absorbance of each sample was read at 450 nm using a Varioskan Flash multimode plate reader. The quantity of VEGF and/or FGF-2 protein was determined against a standard curve.

Quantification of capillary-like structures formation. Matrigel (Corning, USA) was added to 96 well plates that were then kept in a humidified incubator for 30 min. hDMECs were then seeded on the top of the formed gel at a density of $1.3x10^4$ cells/well and incubated for 24 h in a humidified incubator at 37 ºC, 5 % of CO_2 in the presence of filtered VEGF or FGF conditioned media. Negative and positive controls were incubated with DMEM medium or with EndoGRO MV-

VEGF respectively. For the assay using transfected hDFbs, the conditioned media is the same supernatant as was quantified by ELISA. The organization of cells into capillary-like structures was assessed after 24 h after cell staining with Phalloidin-TRITC and DAPI. Micrographs were taken using an Axio Observer inverted Microscope (Zeiss, Germany) with the ZEN Blue 2012 software (Zeiss, Germany). For the assay using conditioned media from cell-laden gene-activated scaffolds, organization in capillary-like structures was assessed using time-lapse imaging. Time-lapse brightfield images were obtained every 30 min over 24 h using an Axio Observer inverted microscope with incubation (37 ºC, 5 % of CO_2), and ZEN Blue 2012 software (Zeiss, Germany). The capillary-like structures formation peak time and half-life were quantified. Peak time corresponds to the period of time required for relevant tubular-like structure formation to be visible, on the other hand, the retention time corresponds to the period of time required upon peak time establishment to achieve tubule regression. Capillary-like structures were screened and an angiogenesis plug-in for ImageJ 1.48[34] was used to quantitatively analyze their formation and organization.

Immunocytochemistry. After fixation, cells were incubated with 1 % Triton X-100 (Sigma-Aldrich, Portugal) for 30 min at RT for permeabilization. Samples were then incubated with mouse anti-human primary antibody CD31 (1:30, Dako, USA) diluted in 1 % BSA solution in PBS for 18 h at 4 ºC. After washing with PBS, samples were incubated for 1 h at RT with the secondary antibody Alexa Fluor 488 donkey anti-mouse (Life Technologies, CA, USA) at a concentration of 1:500 in 1 % BSA solution in PBS. Cytoskeleton and nuclei were counter-stained with Phalloidin-TRITC and DAPI, respectively. Scaffolds were observed using a Leica TCS SP8 confocal microscope (Leica, Germany).

Statistical analysis. GraphPad Prism 8.2.1 software (La Jolla, USA) was used to perform the statistical analysis. The results were compared to a control condition corresponding to non-transfected hDFbs. Data was analyzed using the Shapiro-Wilk normality test. All data followed a normal distribution therefore was analyzed using a two-way ANOVA with Turkey post-test and a one-way ANOVA with Turkey post-test. Significance and confidence were set to 0.05 (95 % of confidence interval), represented by * $p < 0.05$, ** $p < 0.01$, *** $p < 0.001$; **** $p < 0.0001$. All quantitative data refer to 3 independent experiments (n=3) with at least 3 replicates in each condition, in each experiment and are presented as mean ± standard deviation.

Results

Characterization of Ch-pDNA and PEI-pDNA nanoparticles and transfection efficiency on hDFbs

The process of cell transfection starts with complexation between non-viral vectors and plasmids (Figure 1A). The complexation efficiency between Ch or PEI and pVEGF or pFGF2 is shown in Figure 1B. Both pDNA complexes showed high encapsulation efficiency. For Ch, 98.7 % ± 0.7 % and 97.4 % ± 0.5 % were obtained for pVEGF and pFGF-2, respectively. For PEI, 98.5 % ± 1.1 % and 99 % ± 0.7 % efficiency were observed for pVEGF and pFGF2, respectively. Gel electrophoresis (Figure 1C) also confirmed these results, as no bands were observed for both complexed Ch-pDNA and PEI-pDNA, regardless of the pDNA amount. This indicates that the pDNA was strongly complexed with the Ch and PEI.

In order to understand the transfection efficiency of Ch-pGLuc and PEI-pGLuc on hDFbs, luciferase activity was quantified for 14 days (Figure 1E). Luciferase expression peaked at day 3 post-transfection for both non-viral vectors at $7.1x10^5 \pm 3.8x10^5$ versus $3.2x10^5 \pm 4.2x10^5$, with Ch-pGLuc significantly ($p < 0.001$) outperforming PEI-pGLuc. Both non-viral vectors were able to maintain a transient gene expression for 14 days and there were no significant differences on the luciferase expression for the remaining days. Images taken 3-, 7- and 14-days post-transfection show cells expressing GFP, indicating successful transfection of hDFbs (Figure 1D). When quantified (Figure 1F), the transfection efficiency achieved using Ch-pGFP or PEI-pGFP corresponded to 18 % ± 3.5 % and 15 % ± 6.7 % of pGFP-transfected cells, respectively. Significant differences on the number of GFP+ cells were found after 7 days, i.e, Ch-pGFP was higher than PEI-pGFP formulations.

The effect of the Ch-pDNA and PEI-pDNA complexes on hDFbs metabolic activity and proliferation rate was investigated at 3, 7, and 14 days post-transfection with the therapeutic genes pVEGF and/or pFGF2 (Figure 1G). However, right after the transfection the metabolic activity per cells was higher in PEI than in control or Ch, in both pVEGF and pFGF2 conditions (Figure S1). A significant decrease in the metabolic activity of cells transfected with PEI-pVEGF was detected at day 3 when compared to Ch-pVEGF. At day 14, when VEGF was delivered with Ch or PEI, cell metabolic activity showed to be significantly ($p < 0.0001$) higher than the control. No major differences in cell metabolic activity were observed for pFGF2 delivered with Ch or PEI until day 7. At day 14, a significant increase in the metabolic activity ($p < 0.0001$) was achieved for Ch-pFGF2 in relation to control and PEI-pFGF2. The metabolic activity when plasmids were delivered together with Ch was significantly higher ($p < 0.01$) from day 7-onward in comparison with non-transfected cells or PEI. The metabolic activity levels from the dual combination with PEI showed to be similar to the control. The delivery of the non-viral vectors or plasmids alone did not influence negatively cell metabolic activity (Figure S2A).

When DNA content was measured after transfection, a significant decrease in PEI was observed for both pVEGF and pFGF2 conditions (Figure S1). As a marker of cell proliferation (Figure 1H), a significant ($p < 0.01$) decrease up to 14 days was observed when pVEGF is delivered with Ch when compared to control and up to 7 days when compared to PEI. For PEI, only at day 14 post-transfection, a significant ($p < 0.001$) decrease is observed in relation to control. Regarding pFGF2, no significant differences in DNA content were observed until day 14 post-transfection when it was significantly ($p < 0.01$) lower with both vectors in relation to control. Concerning pVEGF and pFGF2 delivered together, the trend observed is the same as pVEGF delivered alone. Plasmids delivered with Ch showed a reduction ($p < 0.01$) in DNA content in all time points when comparing with the control, whereas when plasmids were delivered with PEI, only at day 14 there was a significant ($p < 0.0001$) decrease in DNA content in relation to control. In all time time-points there was also a significant difference ($p < 0.01$) in Ch and PEI,

since plasmids delivered with PEI showed higher DNA content. The delivery of single vectors or plasmids showed a significantly decrease in the amount of DNA content (Figure S2B) in relation

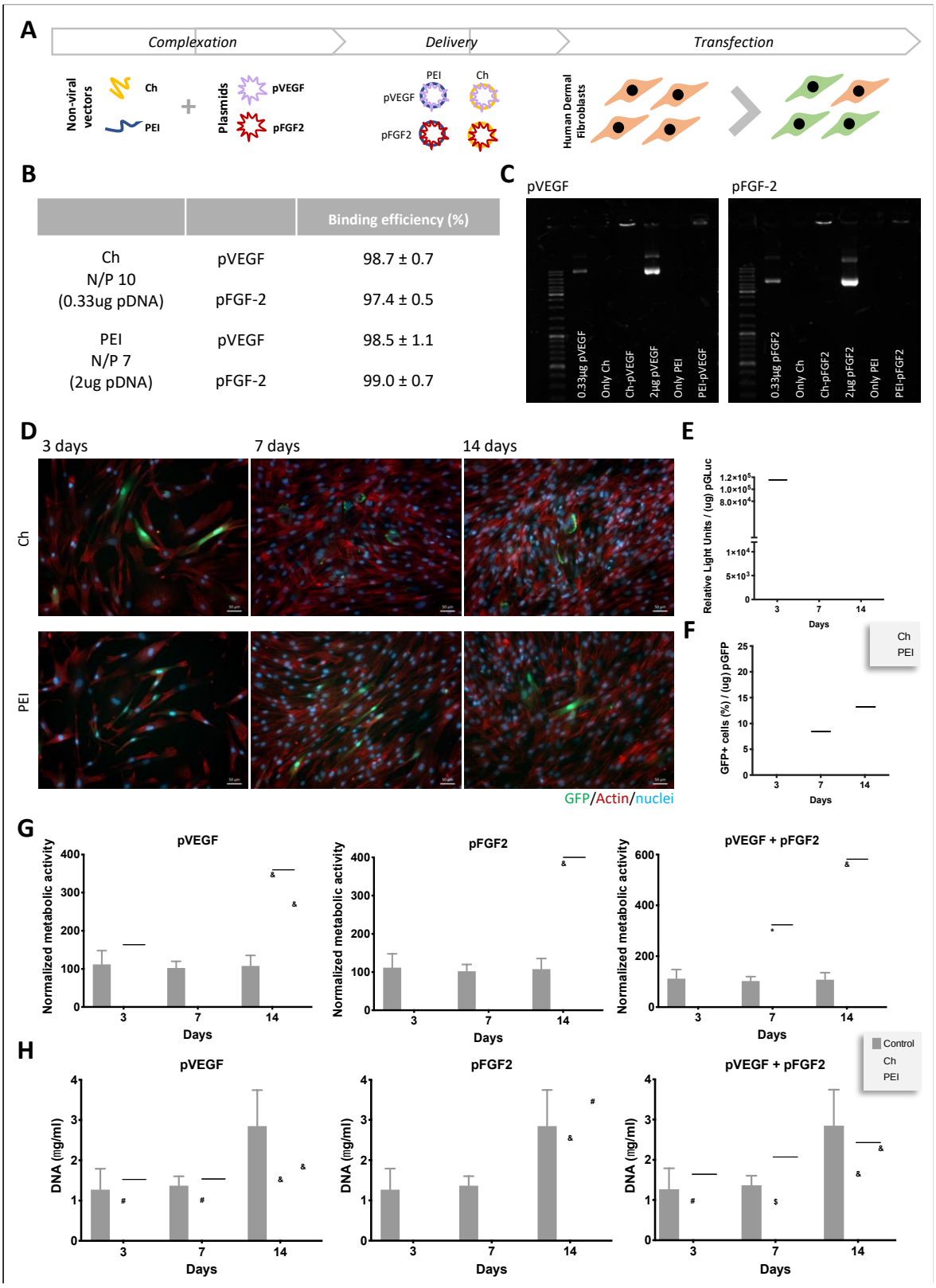

Figure 1. Transfection capability of hDFbs. A) Scheme of non-viral and plasmid complexation that are delivered to human dermal fibroblasts (hDFbs) and leads to cell transfection. B) Binding efficiency of Ch or PEI to pVEGF or pFGF2. C) Complexation of pDNA and the non-viral vectors. From a 1% Agarose gel is possible to observe a complete complexation between Ch or PEI to pVEGF and pFGF2. D) GFP positive cells were visually observable for both formulations at day 3, 7 and 10. Scale bar = 50 μm. E) Transient gene expression of hDFbs using the report system pGLUC showed that Chitosan-pGLuc N/P 10 formulation resulted in a statistically higher level of pGLuc transgene expression in hDFbs compared to PEI-pGLuc N/P 7 formulations at day 3 ($p<0.001$). F) Transfection efficiency in hDFbs using the reporter system pGFP. Both the Chitosan-pGFP N/P 10 (0.33μg pGFP) and PEI-pGFP N/P 7 (2μg pGFP) resulted in a peak transfection efficiency at day 3 of 17.90 ± 3.5% and 15.20 ± 6.7% respectively. G) Metabolic activity was quantified following treatment with Ch- and PEI-pDNA polyplexes. Formulation with pVEGF showed a significant decrease in cell metabolic activity up to day 7 with PEI when compared to control and Ch. H) Cell proliferation by DNA quantification showed a significative decrease over all time-points when pVEGF or pVEGF/pFGF2 were delivered together with Ch. No major differences are observed in pFGF2 conditions up to day 14. Results are expressed as the mean ± standard deviation where n=3, * $p < 0.05$, # $p < 0.01$, $ $p < 0.001$, & $p < 0.0001$ in relation to control (non-transfected hDFbs) or * $p < 0.05$, ** $p < 0.01$, *** $p < 0.001$, **** $p < 0.0001$ in relation to each condition, at each time point.

to control. These results were independent of the vector or

plasmid used. In summary, these results showed that Ch did not impact in cells' metabolic activity but decreased the cell proliferation. In contrast, PEI transfected cells showed lower metabolic activity when compared to Ch but the cell proliferation was similar to non-transfected cells up to day 7.

VEGF and FGF-2 post-transfection therapeutic protein production enhances capillary-like structure formation

The production of VEGF and FGF-2 by pVEGF- and pFGF-2-transfected cells was monitored up to 14 post-transfection (Figure 2A). When pVEGF is delivered to hDFBs with Ch, VEGF protein production peaked at day 3 post-transfection (95.5 pg mL^{-1}). On the other hand, when pVEGF was delivered using PEI, VEGF production peaked at 7 days post-transfection (132.1 pg mL^{-1}). From day 10 onward, the amount of VEGF produced by the control was significantly higher ($p < 0.01$) than the remaining conditions. Regarding the production of FGF-2, both vectors yield significantly higher ($p < 0.0001$) production than the control. The FGF-2 production increased until day 5 when pFGF2 was delivered with Ch, peaking at this time-point (1522.6 pg mL^{-1}). From day 5 until day 10, the FGF-2 production was in a plateau state. pFGF2 delivered with PEI lead to significantly higher ($p < 0.0001$) FGF2 production than the control at day 3 but decreased from that time-point onward.

The ability of 3- and 7-day post-transfection conditioned media from the transfected hDFbs to promote the organization of hDMECs into capillary-like structures was evaluated on matrigel (Figure 2B-C). The 3-day conditioned media of cells transfected with all conditions elicited the formation of capillary-like structures (Figure 2B). Moreover, the quantification of the segments and number of nodes (Figure 2C) showed that the results for transfected cells were significantly ($p < 0.01$) superior than the control, independently of the conditions. The same trend was observed regarding the number of meshes and segments length. With the 7-day conditioned media only cells transfected with pVEGF with Ch or PEI exhibited the formation of capillary-like structures (Figure 2B). However, only with PEI-pVEGF the number of segments and nodes was significantly ($p < 0.01$, $p < 0.05$) higher than the control and Ch-pVEGF (Figure 2C). Together with the ELISA results we conclusively demonstrate that the PEI vector was capable of inducing a superior VEGF therapeutic transgene expression in hDFbs, and the Ch a superior FGF-2 transgene expression. For this reason, for subsequent experiments PEI was used to delivery pVEGF and Ch was used to delivery pFGF-2.

The angiogenic potential of transfected cells in a 3D microenvironment

The angiogenic potential of the transfected hDFbs was evaluated in a 3D microenvironment using hDMECs (Figure 3A) After 3 days in culture, hDMECs adhered to the surface of scaffolds and were in close contact to hDFbs (Figure 3B). Moreover, after 7 days in culture, hDMECs showed the formation of an extensive cell network in both non-transfected and PEI-pVEGF transfected hDFbs. For hDMECs in contact with Ch-pFGF2 and P+C transfected hDFbs presented a more elongated form. These results were independent of the type of scaffold used, as in COL-ChS, COL-HyA and GG-HyA, the same tendency was observed.

The analysis of the supernatant of cultures showed increased secretion of VEGF over time (Figure 4A). The amount of VEGF produced by PEI-pVEGF transfected hDFbs was significantly higher ($p < 0.05$) than the control. Moreover, VEGF levels for PEI-pVEGF transfected hDFbs were significantly superior ($p < 0.0001$) than the dual combination transfection. Residual amounts of VEGF close to P+C were obtained for Ch-pVEGF transfected hDFbs. These results were independent of the type of scaffold used. Quantification of the FGF-2 content showed higher production of FGF-2 at day 3 (Figure 4A) in all scaffolds compared to control. In HyA-containing scaffolds (COL-HyA and GG-HyA), all transfection conditions yield significantly ($p < 0.05$) higher FGF-2 values. In COL-ChS scaffolds significant differences ($p < 0.001$) were observed only for the P+C condition. The overexpression of FGF-2 in relation to control was only maintained over time when cells were transfected with the P+C in the COL scaffolds.

The ability of conditioned medium derived from transfected cells in the 3D environment to induce hDMECs formation capillary-like networks in Matrigel was studied for the different scaffolds (Figure 4B). A significant ($p < 0.05$) early peak time (5h30min) was observed with 3-day COL-HyA conditioned media from co-cultures with hDFbs transfected with PEI-pVEGF, Ch-pFGF2 and P+C (Figure 4Bii), when compared to control (7h30min). Moreover, the retention time of these capillary-like structures were higher ($p < 0.05$) than the control, especially in the case of conditioned media from co-cultures of hDMECs and hDFbs transfected with PEI-pVEGF (7h) and Ch-pFGF2 (7h30min). These findings show that that capillary-like structure formation was faster with 3-day conditioned media from transfected cells and retained the capillaries for a longer time before regression. Additionally, the number of segments produced was significantly ($p < 0.05$) higher in Ch-pFGF2 and P+C conditioned media. With the 7-day COL-HyA conditioned media from the co-cultures, no differences were observed in the capillary-like structures peak time nor retention time. However, a significant ($p < 0.01$) increase in the number of segments was obtained for PEI-pVEGF conditioned media. Regarding COL-ChS and GG-HyA, the significant early peaks and increased number of segments in relation to control occur with the 7-day conditioned media.

Taken together, the results showed higher amounts of VEGF were obtained with PEI-pVEGF 7 days post-transfection while significant higher FGF-2 content was detected in transfected cells 3 days post-transfection. Both these conditions led to a

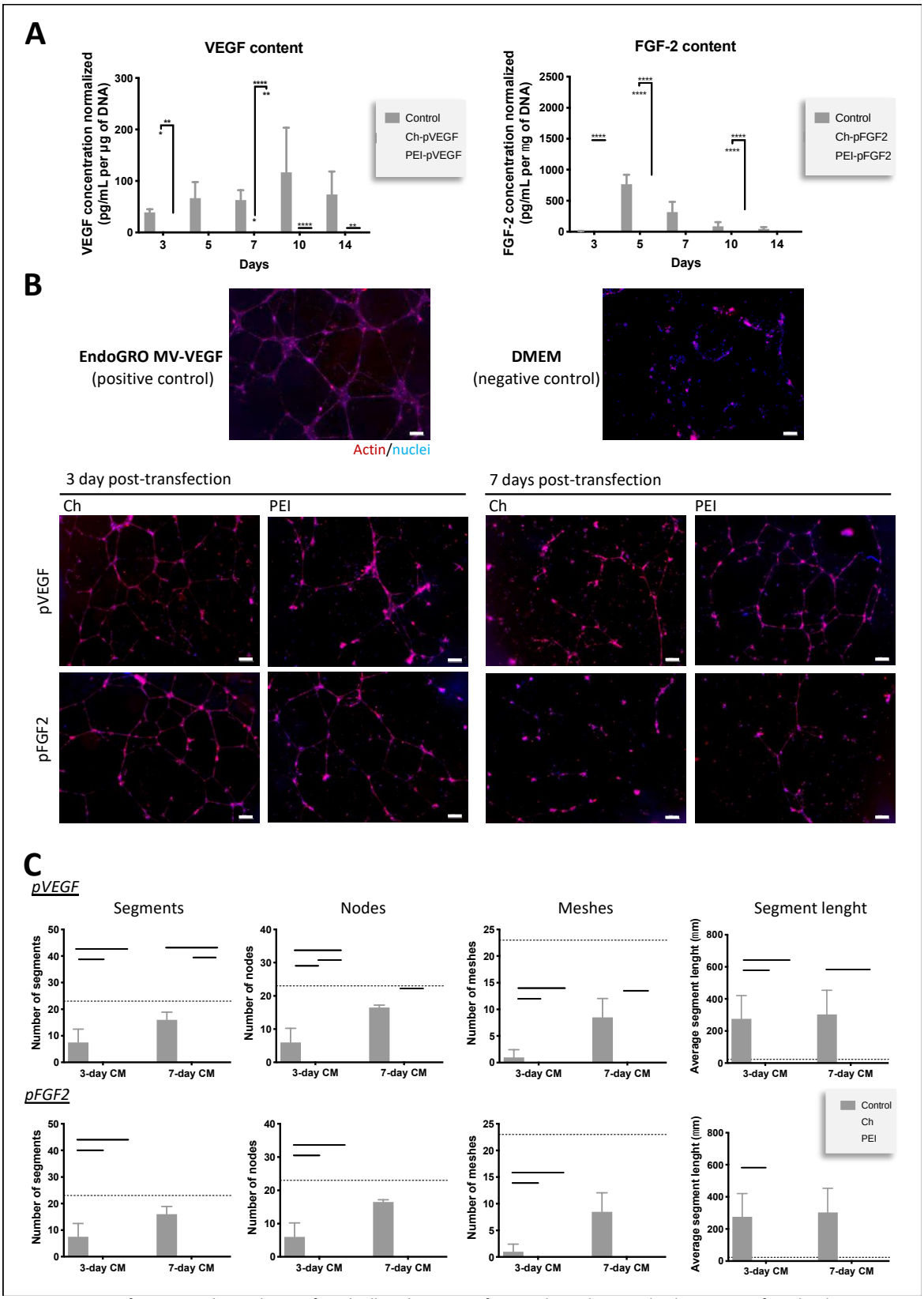

Figure 2. Assessment of protein production by transfected cells and respective functionality on hDMECs. hDFbs were transfected with pVEGF or pFGF2 with Chitosan (0.33 µg dose) or PEI (2 µg dose). A) VEGF and FGF2 proteins were monitored by ELISA at days 3, 5, 7, 10 and 14 post-transfection. Significantly more VEGF protein is produced in Ch-pVEGF at day 3 and PEI-pVEGF at day 7. FGF-2 delivered with Ch showed a significant sustained release up to day 14. Control corresponds to non-transfected hDFbs. B) Tubular-like structures formed by hDMECs cultured on matrigel with conditioned media obtained from representative transfected hDFbs cultures for (i) 3 and (ii) 7 days. After 24h in Matrigel, tubular-like structures were fixed and labelled with Phalloidin-TRITC and DAPI. Controls were made with VEGF-containing EndoGRO (EndoGRO MV-VEGF) which, as expected, stimulated the in vitro formation of capillary-like structures, and with DMEM that did not promote the same. Scale bar = 200 µm. C) Quantification of the number of segments, nodes, meshes and segments lenght present in hDMECs cultured in the presence of the described conditioned media (CM) at day 3 and 7. Control corresponds to hDFbs non-transfected. Matrigel positive control is the horizontal doted line. Results are expressed as mean ± SD where n = 3, * $p < 0.05$, ** $p < 0.01$, *** $p < 0.001$ and **** $p < 0.0001$.

faster formation of capillary-like structures with higher number

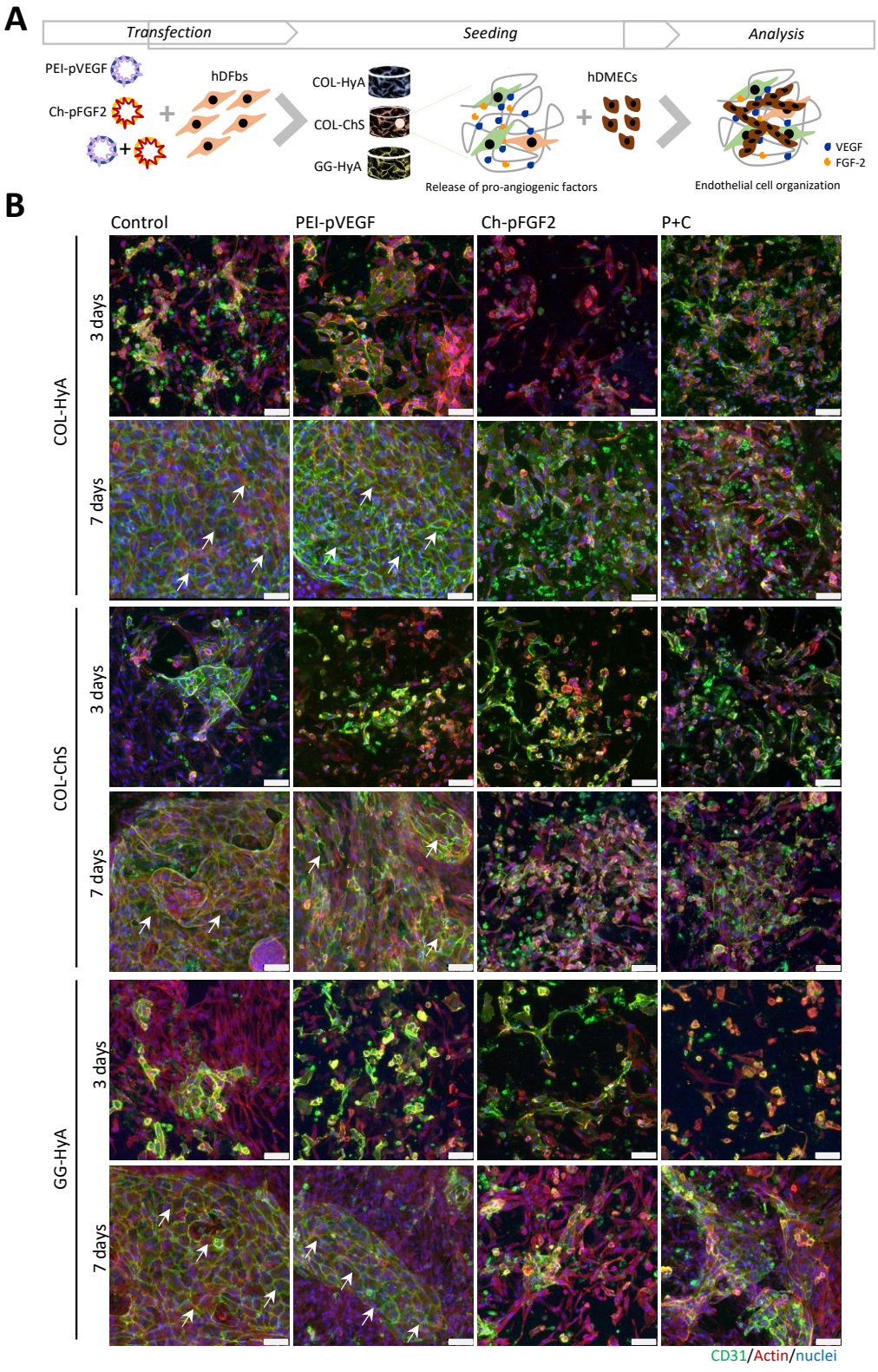

Figure 3. hDMECs organization on COL-GAG and GG-HyA scaffolds after 3 and 7 days. A) Chosen plasmids were delivered to hDFbs and seeded in different scaffolds. The angiogenic capacity of the system is maximized through the release of angiogenic proteins providing a 3D microenvironment for endothelial cells proliferation and organization. B) hDFbs were transfected with PEI-pVEGF, Ch-pFGF2 and the dual combination of both (P+C) and seeded on COL-HyA, COL-ChS and GG-HyA scaffolds with hDMECs. Control correspondes to co-cultures where hDFbs were not transfected. In all scaffolds, co-culture of hDMECs (CD31) with PEI-pVEGF hDFbs showed the formation of an extensive CD31+ endothelial network (white arrows) in all conditions after 7 days. Scale bar: 75 μm.

of segments that were retained for longer periods of time. The dual combination (P+C) showed a downregulation of the production of VEGF and an upregulation of FGF-2. However, the formation of capillary-like structures was also faster than the control and a high number of segments were formed.

Discussion

Growth factors in the form of recombinant proteins have been increasingly used in biomaterial-based strategies to promote vascularization.[35–39] However, the limitations associated with protein delivery, such as high cost, bolus release of proteins, short half-life, and the requirement of high doses to achieve a therapeutic effect[40,41] hinder further developments. Gene therapy might serve as an alternative approach where improved therapeutic responses might be attained due to the sustained protein production over an extended time frame by gene transfected cells. However, the field of gene therapy is typically challenged by the complex regulatory environment with using viral vectors and lack of efficacy with non-viral vectors. We have been working to overcome the challenges with the latter and have shown that when combining transfected cells with scaffolds, besides supporting cell adhesion and proliferation, the scaffold will act to retain the target protein at the site for longer, delaying clearance.[42] Therefore, the hypothesis of this study was that transfected human dermal fibroblasts (hDFbs)-laden scaffolds have their angiogenic capacity maximized through the release of angiogenic factors by the transfected cells. hDFbs were transfected with pro-angiogenic genes, pVEGF and pFGF2, and the effect of these systems on the production of angiogenic factors and formation of vascular-like networks was analysed. VEGF is required for survival, differentiation and formation of networks by endothelial cells,[43] while FGF-2 promotes the endothelial cells sprouting, required at the first steps of the angiogenesis process, also promoting cell-cell interactions required for vessel maturation.[44,45] Since no ideal vector for hDFbs gene transfer had been reported so far, two different gene delivery systems using Ch or PEI were evaluated.[19,22]

Ch- and PEI-pDNA nanoparticles were produced using optimal N/P ratios (N/P 10 for Ch and N/P 7 for PEI) and pDNA doses (0.33 µg and 2 µg, respectively). It was already reported for MSCs that Ch-pDNA formulations do not cause a decrease on cell viability whereas with PEI-pDNA a drop of 40% in the cytotoxicity is obtained.[19] In this present study, none of the Ch-pDNA formulations lead to a decrease in cell viability. Moreover, the metabolic activity of Ch-pDNA formulations from day 10-onward increased 2-fold in relation to control. Interestingly, impairment in cell proliferation was observed for cells transfected with these Ch nanoparticles. Despite the complexion efficiency being over 97 % for both plasmids with Ch, around 3 % of the vectors and plasmids were not complexed. Therefore, while vectors or plasmids delivered alone showed no cytotoxicity, the decrease in DNA content could be caused by the effect of the non-complexed non-viral vector or naked plasmid.[21] On the other hand, PEI–pDNA polyplexes caused cell death in the pVEGF formulation, but did not significantly affected DNA content when compared to control up to 10 days, in agreement with previously published works.[19,21]

When comparing the different non-viral vectors and their transfection efficiency, the results described herein showed that transfected hDFbs were able to maintain a transient gene expression up to 14 days. However, a lower transfection efficiency of hDFbs (15% for PEI and 18% for Ch) was obtained in comparison to what was previously demonstrated for MSCs, where transfection efficiency with Ch-pDNA was approximately 45 %[19,46] and 30 % with PEI-pDNA.[21] Moreover, the Ch-pDNA formulation resulted in a more efficient transgene expression at a lower pDNA dose compared to that of the PEI-pDNA formulation. It has been shown that relatively low transfection efficiencies can facilitate sufficient protein to yield the system functional.[47] For example, Curtin et al (2012) developed a non-viral vector system for bone tissue engineering using nano-hydroxyapatite that had a transfection efficiency of 11 % in MSCs.[47] However, in the same study, when compared to other non-viral vectors with higher transfection efficiencies, the nano-hydroxyapatite-pDNA system produced more BMP-2 protein and consequentially led to higher levels of MSC-mediated osteogenesis in vitro[47] and enhanced bone repair in an in vivo study.[16] In our study, the results show that the production of VEGF and FGF-2 by transfected hDFbs, despite the relatively low transfection efficiency, was translated to enhanced functionality with formation of capillary-like structures, independently of the non-viral vector used. To elucidate the effect and suitability of our system on hDMECs in a 3D microenvironment, these cells were co-cultured with transfected hDFbs in three different scaffolds: COL-HyA, COL-ChS and GG-HyA. After co-culturing the transfected hDFbs with the hDMECs, we noticed that hDMECs were adhering on the top of the hDFbs, keeping close contact with them. Interestingly, hDMECs did not adhere to the scaffold itself despite their composition (containing collagen, chondroitin sulphate or hyaluronic acid) essential for tissue remodelling and angiogenesis. The results indicate that hDMECs only started to form their extensive $CD31^+$ networks after hDFbs spread throughout the scaffolds, suggesting that the ECM secreted factors released by hDFbs were required for their sprouting. This explains why in the Ch-pFGF2 and P+C conditions, the

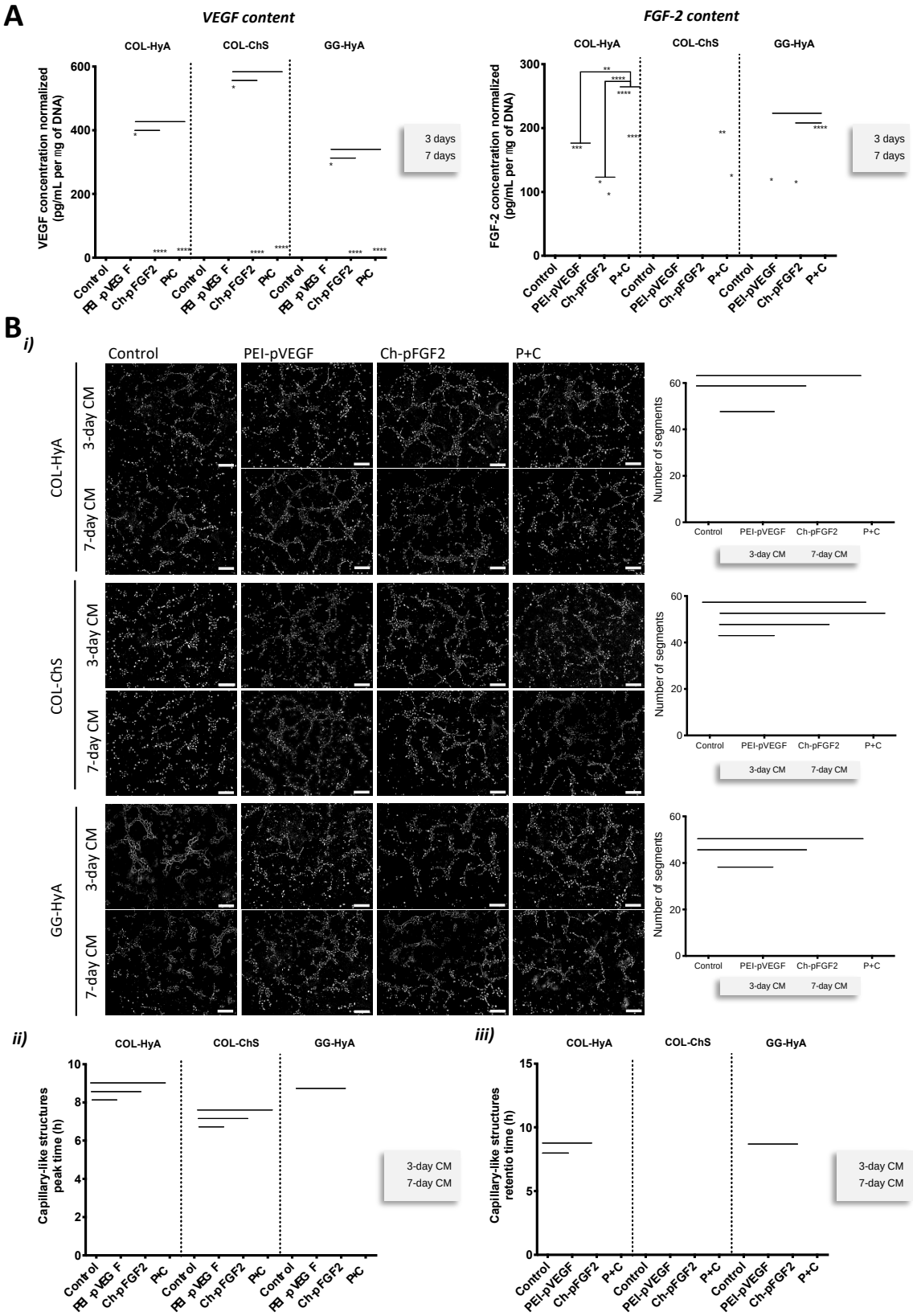

Figure 4. Assessment of the effects of co-cultures of transfected hDFbs and hDMECs in COL-GAG and GG-HyA scaffolds. A) The production of VEGF is significantly higher in the co-cultures control 7 days post-transfection. Regarding FGF-2 content, 3 days after transfection there is a significand increase in protein content on the HyA containing scaffolds (COL-HyA and GG-HyA), when hDFbs are transfected by Ch-pFGF2 and P+C. B) Effect of the conditioned media (CM) of the different scaffolds on hDMECs in a Matrigel assay. (i) Tubular-like structures formed by hDMECs cultured on matrigel with conditioned media obtained from representative transfected hDFbs cultures for 3 and 7 days. Control corresponds to hDFbs non-transfected. Quantification of the number of segments present in hDMECs cultured in the presence of the described conditioned media (CM) at day 3 and 7. (ii) Quantification of the assay showed with 3-day CM, an early peak time of the formation of capillary-like structures as well a (iii) capillary-like structures retention time. Scale bar: 200 μm. Results are expressed as the mean ± standard deviation where n=3, * p<0.05, *** p<0.001, **** p<0.0001 in relation to control.

hDMECs networking is still forming, as suggested by the fact

that hDFbs were still expanding in the 3D microenvironment.

Despite the development of in vitro capillary-like structures being important for in vivo inosculation within a wound, in our current study, only some level of capillary-like structure formation was observed. However, we must give emphases to the importance of non-organized endothelial cells that are present in a construct. In a previous study, we showed an increase in tissue neovascularization, as well as, accelerated wound closure rate and re-epithelization, where endothelial cells, fibroblasts and keratinocytes where seeded in GG-HyA spongy-like hydrogels and implanted in a skin full-thickness wound mice model [27].

Many studies have shown that delivering VEGF or FGF-2 via a scaffold enhances angiogenic response in vivo.[14,48,49] However, due to their short half-life, the factors are degraded and/or cleared from the wound site, often before an effective dose accumulation at the target site. To address this topic, a system combining a scaffold with transfected cells would allow the sustained protein production over an extended time frame. To determine the therapeutic efficacy of our 3D system and to understanding the impact of factors released by the transfected fibroblasts on neighbour endothelial cells, we analysed the bioactivity of the conditioned media taken from transfected hDFbs-seeded scaffolds by assessing functionality in hDMECs. In all of these systems, the higher amounts of VEGF were obtained with PEI-pVEGF 7 days post-transfection. Moreover, the conditioned media from the PEI-pVEGF led to a faster formation of capillary-like structures with higher number of segments that were retained for longer periods of time. These results were in concordance with the observations in 2D experiments, since the activity of the system was greater when pVEGF was delivered with PEI. In contrast, a significantly higher FGF-2 content was detected in transfected cells in comparison to non-transfected cells 3 days post-transfection. The amount of FGF-2 that was produced resulted in faster and earlier formation of capillary-like structures with a significant increase in the number of segments with 3-day conditioned media. The results remained consistent with the experiments carried out in 2D, where a significant higher number of segments were formed with conditioned media from Ch-pFGF2. Interestingly, in the 3D experiments, cells transfected with pVEGF also showed higher production of the growth factor in relation to non-transfected cells. Moreover, the protein amount produced in all our 3D systems equate to mere fractions of the amount of recombinant human VEGF[50] and FGF-2[51,52] that are routinely delivered in the clinic in order to achieve a therapeutic effect. Furthermore, we demonstrated that our platform can be successfully applied to different scaffolds, leading to maximized angiogenic capacity through the transient release of angiogenic factors by transfected hDFbs. Envisioning the immediate application of our systems as a dermal construct to support skin vascularization and regeneration, an early effect on vascularization promoting its integration is expected, as both angiogenic factors production would be beneficial to support early endothelial cell response. Moreover, the FGF-2 production up to 14 days is expected to induce fibroblast proliferation and impair the phenotypical switch of fibroblasts to myofibroblasts to achieve a less scar [53,54]. Notwithstanding, this system can also be translated into a wide variety of applications for tissue engineering and beyond, such as, pathophysiology studies, models of disease, culture systems and drug screening, or any structure where vasculature is requires for regeneration.

Considering the potential synergistic effect of VEGF and FGF-2 on neovascular formation,[55–58] the concomitant delivery of pVEGF and pFGF2 (P+C) was analysed. To our knowledge, there are no other examples of the dual delivery of pVEGF and pFGF2 within a tissue engineering scaffold. The results for the dual combination showed a downregulation of the production of VEGF and an upregulation of FGF-2. These results were not exclusive for this system, since in fact, only residual amounts of VEGF were detected when hDFbs were transfected with single Ch-pFGF2. Moreover, with single PEI-pVEGF transfections, an upregulation of FGF-2 was confirmed. This could explain why the dual combination led to a downregulation of VEGF but an upregulation of FGF-2 when compared to single transfections. These results highlighted the efficiency of the gene-activated cells but do not uphold upon the synergistic effect of VEGF and FGF-2 in the co-cultures. This could result from different pathways being used by cells to internalize the nanoparticles. PEI-pDNA polyplexes enter in the cell via clathrin- or caveolae-mediated endocytosis.[59] However, PEI polyplexes that are internalized via clathrin-mediated endocytosis are then targeted to the lysosomal compartment. Polyplexes taken up exclusively via caveolae do not reach this compartment and the transfection becomes more efficient.[59] Others hypothesized that only pDNA entering the cell by caveolae-mediated uptake of the polyplexes escapes the lysosomal destination and can become transfection-effective,[59] despite the consensus that PEI polyplexes are taken up by the two mechanisms.[60] Interestingly, Ch-pDNA are reported to enter cells only via the caveolae route of endocytosis.[61] By negatively attracting charged ions into the endosome, they cause rupture of this biological compartment enabling the release of the polyplexes into the cytoplasm, a mechanism called “proton-sponge” effect.[62–64] Since both pDNA complexes with non-viral vectors can enter cells via caveolae-mediated endocytosis, we assume that cells are prioritizing Ch-pDNA nanoparticles due to their lower size (~109nm vs ~150nm) which leads to almost non-production of VEGF and the upper-regulation of FGF-2. These results suggest that future strategies could involve the separate transfection of each vector followed by seeding on the same scaffold thus increasing its yield.

Conclusions

In summary, hDFbs were successfully transfected with Ch- and PEI-pDNA. Despite low transfection efficiency, an increased production of functional VEGF and FGF-2 was obtained with almost no impairment in cell metabolic activity. Moreover, those studies also showed that in order to have a superior VEGF and FGF-2 transgene expression and thus formation of capillary-like structures, pVEGF should be delivered with PEI and pFGF2 with Ch. Furthermore, co-culture of hDMECs and transfected hDFbs comprising PEI-pVEGF (P), Ch-pFGF2 (C) or the

combination (P+C) in the scaffolds showed formation of an extensive endothelial cell network in non-transfected and PEI-pVEGF transfected hDFbs conditions. However, when evaluating the overall effect of the system in an external assay with hDMECs that were not directly in contact with transfected hDFbs, greater, faster and higher retention time of thee formed capillary-like structures were observed when VEGF and FGF-2 were delivered and produced separately when compared to non-transfected and P+C conditions. We believe that these cell-laden matrices offer a novel, selective and alternative approach to developed vascularized tissue engineered constructs, providing also a new set of tools for pathophysiology studies, models of disease, culture systems and drug screening. The next step will be to evaluate their performance in an in vivo model.

Conflicts of interest

There are no conflicts to declare.

Acknowledgements

This work was supported by GENE2SKIN Twinning Project (692221) Horizon 2020 (European Commission), Dressing4Scars M-ERA-NET2/0013/2016 (APM, FJO), NORTE-08-5369-FSE-000037 (HRM), Health Research Board ILP-POR-2017-032 (RMR) and The Discoveries Centre for Regenerative and Precision Medicine H2020-WIDESPREAD-2014-1-739572. The authors would also like to acknowledge Andreia Carvalho and Raquel Ribeiro for the support on the experimental assays.

References

1 G. M. Mitchell and W. A. Morrison, in *Vascularization for Tissue Engineering and Regenerative Medicine*, 2017.

2 J. Rouwkema, N. C. Rivron and C. A. van Blitterswijk, Vascularization in tissue engineering, *Trends Biotechnol.*, 2008, **26**, 434–441.

3 M. Lovett, K. Lee, A. Edwards and D. L. Kaplan, Vascularization strategies for tissue engineering., *Tissue Eng. Part B. Rev.*, 2009, **15**, 353–70.

4 X. Sun, W. Altalhi and S. S. Nunes, Vascularization strategies of engineered tissues and their application in cardiac regeneration, *Adv. Drug Deliv. Rev.*, 2016, **96**, 183–194.

5 L. P. D. Silva, R. P. Pirraco, T. C. Santos, R. Novoa-Carballal, M. T. Cerqueira, R. L. Reis, V. M. Correlo and A. P. Marques, Neovascularization Induced by the Hyaluronic Acid-Based Spongy-Like Hydrogels Degradation Products, *ACS Appl. Mater. Interfaces*, 2016, **8**, 33464–33474.

6 G. Yang, B. Mahadik, J. Y. Choi and J. P. Fisher, Vascularization in tissue engineering: fundamentals and state-of-art, *Prog. Biomed. Eng.*, 2020, **2**, 012002.

7 R. Montesano, M. S. Pepper and L. Orci, Paracrine induction of angiogenesis in vitro by Swiss 3T3 fibroblasts, *J. Cell Sci.*, 1993, **105**, 1013–24.

8 O. C. Velazquez, R. Snyder, Z. J. Liu, R. M. Fairman and M. Herlyn, Fibroblast-dependent differentiation of human microvascular endothelial cells into capillary-like 3-dimensional networks, *FASEB J.*, 2002, **16**, 1316–8.

9 T. A. Martin, K. G. Harding and W. G. Jiang, Regulation of angiogenesis and endothelial cell motility by matrix-bound fibroblasts, *Angiogenesis*, 1999, **3**, 69–76.

10 M. J. Cross and L. Claesson-Welsh, FGF and VEGF function in angiogenesis: Signalling pathways, biological responses and therapeutic inhibition, *Trends Pharmacol. Sci.*, 2001, **22**, 201–7.

11 A. C. Newman, M. N. Nakatsu, W. Chou, P. D. Gershon and C. C. W. Hughes, The requirement for fibroblasts in angiogenesis: fibroblast-derived matrix proteins are essential for endothelial cell lumen formation, *Mol. Biol. Cell*, 2011, **22**, 3791–800.

12 C. Cam, S. Zhu, N. F. Truong, P. O. Scumpia and T. Segura, Systematic evaluation of natural scaffolds in cutaneous wound healing, *J. Mater. Chem. B*, 2015, **3**, 7986–7992.

13 I. Wilcke, J. A. Lohmeyer, S. Liu, A. Condurache, S. Krüger, P. Mailänder and H. G. Machens, VEGF165 and bFGF protein-based therapy in a slow release system to improve angiogenesis in a bioartificial dermal substitute in vitro and in vivo, *Langenbeck's Arch. Surg.*, 2007, **392**, 305–14.

14 L. W, L. Y, G. R, Z. Y, X. W and Z. Y, In Vitro and in Vivo Evaluation of a Novel collagen/cellulose Nanocrystals Scaffold for Achieving the Sustained Release of Basic Fibroblast Growth Factor, *J. Biomater. Appl.*, 2015, **29**, 882–893.

15 Q. Liu, Y. Huang, Y. Lan, Q. Zuo, C. Li, Y. Zhang, R. Guo and W. Xue, Acceleration of skin regeneration in full-thickness burns by incorporation of bFGF-loaded alginate microspheres into a CMCS–PVA hydrogel, *J. Tissue Eng. Regen. Med.*, 2017, **11**, 1562–1573.

16 C. M. Curtin, E. G. Tierney, K. Mcsorley, S. A. Cryan, G. P. Duffy and F. J. O'Brien, Combinatorial gene therapy accelerates bone regeneration: Non-viral dual delivery of VEGF and BMP2 in a collagen-nanohydroxyapatite scaffold, *Adv. Healthc. Mater.*, 2015, **4**, 223–7.

17 R. Lugano, M. Ramachandran and A. Dimberg, Tumor angiogenesis: causes, consequences, challenges and opportunities, *Cell. Mol. Life Sci.*, 2019, **77**, 1745–1770.

18 J. Kim, A. C. Mirando, A. S. Popel and J. J. Green, Gene delivery nanoparticles to modulate angiogenesis, *Adv. Drug Deliv. Rev.*, 2017, **119**, 20–43.

19 R. M. Raftery, E. G. Tierney, C. M. Curtin, S. A. Cryan and F. J. O'Brien, Development of a gene-activated scaffold platform for tissue engineering applications using chitosan-pDNA nanoparticles on collagen-based scaffolds, *J. Control. Release*, 2015, **210**, 84–94.

20 R. M. Raftery, I. Mencía Castaño, G. Chen, B. Cavanagh, B. Quinn, C. M. Curtin, S. A. Cryan and F. J. O'Brien, Translating the role of osteogenic-angiogenic coupling in bone formation: Highly efficient chitosan-pDNA activated scaffolds can accelerate bone regeneration in critical-sized bone defects, *Biomaterials*, 2017, **149**, 116–127.

21 E. G. Tierney, G. P. Duffy, A. J. Hibbitts, S. A. Cryan and F. J. O'Brien, The development of non-viral gene-activated matrices for bone regeneration using polyethyleneimine (PEI) and collagen-based scaffolds, *J. Control. Release*, 2012, **158**, 304–311.

22 E. G. Tierney, K. McSorley, C. L. Hastings, S. A. Cryan, T. O'Brien, M. J. Murphy, F. P. Barry, F. J. O'Brien and G. P. Duffy, High levels of ephrinB2 over-expression increases the osteogenic differentiation of human mesenchymal stem cells and promotes enhanced cell mediated mineralisation in a polyethyleneimine-ephrinB2 gene-activated matrix, *J. Control. Release*, 2013, **165**, 173–82.

23 F. J. O'Brien, B. a. Harley, I. V. Yannas and L. Gibson, Influence of freezing rate on pore structure in freeze-dried collagen-GAG scaffolds, *Biomaterials*, 2004, **25**, 1077–1086.

24 F. J. O'Brien, B. A. Harley, I. V. Yannas and L. J. Gibson, The effect of pore size on cell adhesion in collagen-GAG scaffolds, *Biomaterials*, 2005, **26**, 433–441.

25 L. P. da Silva, M. T. Cerqueira, R. a. Sousa, R. L. Reis, V. M. Correlo and A. P. Marques, Engineering cell-adhesive gellan gum spongy-like hydrogels for regenerative medicine purposes, *Acta Biomater.*, 2014, **10**, 4787–4797.

26 WO2014167513 (A1), 2014.

27 M. T. Cerqueira, L. P. Da Silva, T. C. Santos, R. P. Pirraco, V. M. Correlo, A. P. Marques and R. L. Reis, Human skin cell fractions fail to self-organize within a gellan gum/hyaluronic acid matrix but positively influence early wound healing, *Tissue Eng. - Part A*, 2014, **20**, 1369–78.

28 A. Matsiko, T. J. Levingstone, F. J. O'Brien and J. P. Gleeson, Addition of hyaluronic acid improves cellular infiltration and promotes early-stage chondrogenesis in a collagen-based scaffold for cartilage tissue engineering, *J. Mech. Behav. Biomed. Mater.*, 2012, **11**, 41–52.

29 E. L. Pardue, S. Ibrahim and A. Ramamurthi, Role of hyaluronan in angiogenesis and its utility to angiogenic tissue engineering., *Organogenesis*, 2008, **4**, 203–14.

30 J. Sambrook, E. F. Fritsch and T. Maniatis, *Molecular Cloning. A laboratory manual.*, Cold Spring Harbor Laboratory, 1989.

31 J. B. Lepecq and C. Paoletti, A fluorescent complex between ethidium bromide and nucleic acids. Physical-Chemical characterization, *J. Mol. Biol.*, 1967, **27**, 87–106.

32 M. T. Cerqueira, L. P. Da Silva, T. C. Santos, R. P. Pirraco, V. M. Correlo, R. L. Reis and A. P. Marques, Gellan gum-hyaluronic acid spongy-like hydrogels and cells from adipose tissue synergize promoting neoskin vascularization, *ACS Appl. Mater. Interfaces*, 2014, **6**, 19668–79.

33 L. P. da Silva, A. K. Jha, V. M. Correlo, A. P. Marques, R. L. Reis and K. E. Healy, Gellan Gum Hydrogels with Enzyme-Sensitive Biodegradation and Endothelial Cell Biorecognition Sites, *Adv. Healthc. Mater.*, 2018, **7**, 1700686.

34 G. Carpentier, M. Martinelli, J. Courty and I. Cascone, Angiogenesis Analyzer for ImageJ, *4th ImageJ User Dev. Conf.*, 2012, 198–201.

35 J. W. Park, S. R. Hwang and I. S. Yoon, Advanced Growth Factor Delivery Systems in Wound Management and Skin Regeneration, *Molecules*, 2017, **22**, 1259.

36 A. Yu, H. Niiyama, S. Kondo, A. Yamamoto, R. Suzuki and Y. Kuroyanagi, Wound dressing composed of hyaluronic acid and collagen containing EGF or bFGF: Comparative culture study, *J. Biomater. Sci. Polym. Ed.*, 2013, **24**, 1015–26.

37 R. Mittermayr, T. Morton, M. Hofmann, S. Helgerson, M. Van Griensven and H. Redl, Sustained (rh)VEGF165 release from a sprayed fibrin biomatrix induces angiogenesis, up-regulation of endogenous VEGF-R2, and reduces ischemic flap necrosis, *Wound Repair Regen.*, 2008, **16**, 542–50.

38 K. Mizuno, K. Yamamura, K. Yano, T. Osada, S. Saeki, N. Takimoto, T. Sakurai and Y. Nimura, Effect of chitosan film containing basic fibroblast growth factor on wound healing in genetically diabetic mice, *J. Biomed. Mater. Res. - Part A*, 2003, **64**, 177–81.

39 P. Losi, E. Briganti, C. Errico, A. Lisella, E. Sanguinetti, F. Chiellini and G. Soldani, Fibrin-based scaffold incorporating VEGF- and bFGF-loaded nanoparticles stimulates wound healing in diabetic mice, *Acta Biomater.*, 2013, **9**, 7814–21.

40 H. Storrie and D. J. Mooney, Sustained delivery of plasmid DNA from polymeric scaffolds for tissue engineering, *Adv. Drug Deliv. Rev.*, 2006, **58**, 500–14.

41 D. W. Pack, A. S. Hoffman, S. Pun and P. S. Stayton, Design and development of polymers for gene delivery, *Nat. Rev. Drug Discov.*, 2005, **4**, 581–593.

42 R. M. Raftery, E. G. Tierney, C. M. Curtin, S.-A. Cryan and F. J. O'Brien, Development of a gene-activated scaffold platform for tissue engineering applications using chitosan-pDNA nanoparticles on collagen-based scaffolds, *J. Control. Release*, 2015, **210**, 84–94.

43 L. A. Kunz-Schughart, J. A. Schroeder, M. Wondrak, F. Van Rey, K. Lehle, F. Hofstaedter and D. N. Wheatley, Potential of fibroblasts to regulate the formation of three-dimensional vessel-like structures from endothelial cells in vitro, *Am. J. Physiol. - Cell Physiol.*, 2006, **290**, C1385-98.

44 P. A. Underwood, P. A. Bean and J. R. Gamble, Rate of endothelial expansion is controlled by cell:cell adhesion, *Int. J. Biochem. Cell Biol.*, 2002, **34**, 55–69.

45 M. Presta, P. Dell'Era, S. Mitola, E. Moroni, R. Ronca and M. Rusnati, Fibroblast growth factor/fibroblast growth factor receptor system in angiogenesis, *Cytokine Growth Factor Rev.*, 2005, **16**, 159–78.

46 R. Raftery, F. J. O'Brien and S. A. Cryan, Chitosan for gene delivery and orthopedic tissue engineering applications, *Molecules*, 2013, **18**, 5611–5647.

47 C. M. Curtin, G. M. Cunniffe, F. G. Lyons, K. Bessho, G. R. Dickson, G. P. Duffy and F. J. O'Brien, Innovative collagen nano-hydroxyapatite scaffolds offer a highly efficient non-viral gene delivery platform for stem cell-mediated bone formation, *Adv. Mater.*, 2012, **24**, 749–54.

48 B. Li, H. Wang, G. Zhou, J. Zhang, X. Su, Z. Huang, Q. Li, Z. Wu and G. Qiu, VEGF-loaded biomimetic scaffolds: a promising approach to improve angiogenesis and osteogenesis in an ischemic environment, *RSC Adv.*, 2017, **7**, 4253–4259.

49 I. Wilcke, J. Lohmeyer, S. Liu, A. Condurache, S. Krüger, P. Mailänder and H. Machens, VEGF(165) and bFGF Protein-Based Therapy in a Slow Release System to Improve Angiogenesis in a Bioartificial Dermal Substitute in Vitro and in Vivo, *Langenbeck's Arch. Surg.*, 2007, **392**, 305–14.
50 J. R. Hanft, R. A. Pollak, A. Barbul, C. van Gils, P. S. Kwon, S. M. Gray, C. J. Lynch, C. P. Semba and T. J. Breen, Phase I trial on the safety of topical rhVEGF on chronic neuropathic diabetic foot ulcers, *J. Wound Care*, 2008, **17**, 30–2.
51 M. C. Robson, D. P. Hill, P. D. Smith, X. Wang, K. Meyer-Siegler, F. Ko, J. S. VandeBerg, W. G. Payne, D. Ochs and L. E. Robson, Sequential cytokine therapy for pressure ulcers: Clinical and mechanistic response, *Ann. Surg.*, 2000, **231**, 600–611.
52 T. Ohura, T. Nakajo, T. Moriguchi, H. Oka, M. Tachi, N. Ohura, R. Nogami and S. Murayama, Clinical efficacy of basic fibroblast growth factor on pressure ulcers: Case-control pairing study using a new evaluation method, *Wound Repair Regen.*, 2011, **19**, 542–51.
53 S. Tiede, N. Ernst, A. Bayat, R. Paus, V. Tronnier and C. Zechel, Basic fibroblast growth factor: A potential new therapeutic tool for the treatment of hypertrophic and keloid scars, *Ann. Anat.*, 2009, **191**, 33–44.
54 S. Akita, K. Akino and A. Hirano, Basic Fibroblast Growth Factor in Scarless Wound Healing, *Adv. Wound Care*, 2013, **2**, 44–49.
55 M. S. Pepper, N. Ferrara, L. Orci and R. Montesano, Potent synergism between vascular endothelial growth factor and basic fibroblast growth factor in the induction of angiogenesis in vitro, *Biochem. Biophys. Res. Commun.*, 1992, **189**, 824–31.
56 F. Goto, K. Goto, K. Weindel and J. Folkman, Synergistic effects of vascular endothelial growth factor and basic fibroblast growth factor on the proliferation and cord formation of bovine capillary endothelial cells within collagen gels, *Lab. Investig.*, 1993, **69**, 508–17.
57 T. Asahara, C. Bauters, L. P. Zheng, S. Takeshita, S. Bunting, N. Ferrara, J. F. Symes and J. M. Isner, Synergistic effect of vascular endothelial growth factor and basic fibroblast growth factor on angiogenesis in vivo, *Circulation*, 1995, **92**, II365-71.
58 M. R. Kano, Y. Morishita, C. Iwata, S. Iwasaka, T. Watabe, Y. Ouchi, K. Miyazono and K. Miyazawa, VEGF-A and FGF-2 synergistically promote neoangiogenesis through enhancement of endogenous PDGF-B-PDGFRβ signaling, *J. Cell Sci.*, 2005, **118**, 3759–68.
59 J. Rejman, A. Bragonzi and M. Conese, Role of clathrin- and caveolae-mediated endocytosis in gene transfer mediated by lipo- and polyplexes, *Mol. Ther.*, 2005, **12**, 468–74.
60 T. Bieber, W. Meissner, S. Kostin, A. Niemann and H. P. Elsasser, Intracellular route and transcriptional competence of polyethylenimine-DNA complexes, *J. Control. Release*, 2002, **82**, 441–54.
61 Z. Garaiova, S. P. Strand, N. K. Reitan, S. Lélu, S. T. Størset, K. Berg, J. Malmo, O. Folasire, A. Bjørkøy and C. De L. Davies, Cellular uptake of DNA-chitosan nanoparticles: The role of clathrin- and caveolae-mediated pathways, *Int. J. Biol. Macromol.*, 2012, **51**, 1043–51.
62 J.-P. Behr, The Proton Sponge: a Trick to Enter Cells the Viruses Did Not Exploit, *Chimia (Aarau).*, 1997, **51**, 34–36.
63 W. Liang and J. K. W. Lam, in *Molecular Regulation of Endocytosis*, ed. B. Ceresa, IntechOpen, 2012.
64 R. M. Raftery, D. P. Walsh, I. M. Castaño, A. Heise, G. P. Duffy, S. A. Cryan and F. J. O'Brien, Delivering Nucleic-Acid Based Nanomedicines on Biomaterial Scaffolds for Orthopedic Tissue Repair: Challenges, Progress and Future Perspectives, *Adv. Mater.*, 2016, **28**, 5447–69.